

## ARTICLES

## Size criterion for amorphization of molecular ionic solids

G. Serghiou

*Max-Planck Institute for Chemistry, Postfach 3060, 55020 Mainz, Germany*

H.-J. Reichmann

*Bayerisches Geoinstitut, Universitaet Bayreuth, Universitaetsstrasse 30, 95440 Bayreuth, Germany*

R. Boehler

*Max-Planck Institute for Chemistry, Postfach 3060, 55020 Mainz, Germany*

(Received 16 January 1997)

X-ray-diffraction measurements show that  $\text{Rb}_2\text{ZnBr}_4$ ,  $\text{K}_2\text{ZnCl}_4$ , and  $\text{Rb}_2\text{ZnCl}_4$  become amorphous at pressures exceeding 10 GPa. In contrast, their  $\text{Cs}_2\text{ZnCl}_4$  and  $\text{K}_2\text{SeO}_4$  isomorphs undergo crystal-crystal phase transitions and do not amorphize at the highest pressures measured  $\sim 60$  GPa. This indicates that the tendency of  $A_2BX_4$  molecular ionic solids to amorphize upon compression depends predominantly on the ratio of the size of the anionic tetrahedral  $BX_4$  groups to that of the interstitial  $A$  cations. This criterion is also consistent with the incommensurate phase behavior exhibited by several of these solids at ambient pressure. [S0163-1829(97)05022-4]

## I. INTRODUCTION

Identifying structural relationships between the crystalline and noncrystalline state is of fundamental interest in materials research.<sup>1</sup> Pressure-induced crystalline to noncrystalline transitions have therefore been the focus of intense study because the amorphous state produced at room temperature involves only small displacements in the atomic positions of the ambient pressure crystal. This phenomenon has now been observed for all classes on bonding.<sup>2-10</sup> A central question in the study of these crystalline to noncrystalline transitions is "What basic structural feature of a crystal dictates its tendency to amorphize upon compression?" We address this question here for the case of  $A_2BX_4$  molecular ionic solids (Fig. 1, Table I) through a comparative examination of the pressure-induced transformations of six isomorphs within this family, namely,  $\text{K}_2\text{ZnCl}_4$ ,  $\text{Rb}_2\text{ZnCl}_4$ ,  $\text{Cs}_2\text{ZnCl}_4$ ,  $\text{Cs}_2\text{ZnBr}_4$ ,  $\text{Rb}_2\text{ZnBr}_4$ , and  $\text{K}_2\text{SeO}_4$ . In their normal ambient pressure paraelectric phase these insulating crystals are orthorhombic with  $Pnma$  space group and have four formula units per unit cell. They consist of anionic  $BX_4$  tetrahedral groups which are separated from each other by interstitial  $A$  cations.<sup>11-16</sup> The essential way in which these systems differ from each other is via the ratios of the sizes of the anionic  $BX_4$  tetrahedral units to that of their interstitial  $A$  cations ( $\text{ZnCl}_4/\text{K}^+ = 1.69$ ,  $\text{ZnBr}_4/\text{Rb}^+ = 1.62$ ,  $\text{ZnCl}_4/\text{Rb}^+ = 1.52$ ,  $\text{ZnBr}_4/\text{Cs}^+ = 1.43$ ,  $\text{ZnCl}_4/\text{Cs}^+ = 1.35$ ,  $\text{SeO}_4/\text{K}^+ = 1.23$ ). Therefore we can directly examine the importance of this size ratio in influencing crystalline to noncrystalline transitions within this family.

## II. EXPERIMENTAL DETAILS

We monitored the transformations using a diamond cell and energy-dispersive x-ray diffraction at the Hamburg

High Energy Synchrotron Source using a Ge solid-state detector.  $E_d$  ranged from 68 to 80 keV  $\text{\AA}$  and the beam was collimated to  $40 \times 40 \mu\text{m}$ . Measurements were performed on fine-grained samples placed in  $150 \mu\text{m}$  diameter gasket holes. These salts are soft so they could effectively act as their own pressure medium. Nevertheless the observed pressure-induced amorphizations of  $\text{Rb}_2\text{ZnCl}_4$  and  $\text{K}_2\text{ZnCl}_4$  were measured both with and without an argon medium (Fig. 2) completely surrounding pressed powder pellets confirming that the order-disorder transitions were a pure structural effect, i.e., not caused by any shear in the sample. Ruby fluorescence, the diffraction lines of argon or those of gold were used to monitor the pressure.<sup>17-19</sup> The samples were characterized at ambient pressure using x-ray diffraction and Raman spectroscopy. The patterns of the six isomorphs agreed with those reported in the literature.<sup>16,20</sup>

## III. RESULTS

We focus first on the three chloride isomorphs. The principal observation to make about the effect of pressure on the

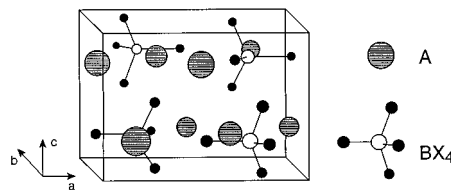


FIG. 1. Schematic of the experimentally determined average structure of  $A_2BX_4$  molecular ionic crystals ( $A = \text{K}, \text{Rb}, \text{Cs}$ ;  $B = \text{Zn}, \text{Se}, \text{Cr}, \text{S}, \text{Cd}$ ;  $X = \text{Cl}, \text{Br}, \text{I}, \text{O}$ ) in their orthorhombic  $Pnma$  phase. The interstitial sites between the isolated anionic tetrahedral  $BX_4$  units are filled with  $A$  cations (grey balls). The white balls represent  $B$  cations and the black balls designate  $X$  anions (Ref. 16).

TABLE I. An illustrative list of  $A_2BX_4$  compounds as a function of the ratio  $(r_B + r_X)/r_A$ , where  $r_i$  are the ionic radii (Refs. 14 and 16). The average experimental value for the distance  $B-X$  in the  $BX_4$  tetrahedra was taken as  $r_B + r_X$ . The systems examined in this study are depicted with bold lettering.

$A_2BX_4$	$BX_4/A$
$K_2CoCl_4$	1.702
$K_2ZnBr_4$	1.695
<b><math>K_2ZnCl_4</math></b>	1.691
$Cs_2CdI_4$	1.653
<b><math>Rb_2ZnBr_4</math></b>	1.616
$Rb_2CoBr_4$	1.603
$Cs_2HgBr_4$	1.563
$Cs_2ZnI_4$	1.550
$Cs_2CdBr_4$	1.550
$Rb_2CoCl_4$	1.527
<b><math>Rb_2ZnCl_4</math></b>	1.521
$Cs_2HgCl_4$	1.490
<b><math>Cs_2ZnBr_4</math></b>	1.431
<b><math>Cs_2ZnCl_4</math></b>	1.347
$K_2CrO_4$	1.236
<b><math>K_2SeO_4</math></b>	1.225
$Rb_2SeO_4$	1.104
$Cs_2SeO_4$	0.974

x-ray-diffraction patterns of the three isomorphs is their very similar behavior at low pressures and their sharply contrasting behavior at high pressure [Figs. 3(a)–3(c)]. At low pressures all diffraction peaks shift to higher energies and the x-ray patterns develop a clustering of peaks, (depicted by arrows in the figures), signaling a phase transformation. At higher pressures for the case of  $K_2ZnCl_4$  and  $Rb_2ZnCl_4$  pronounced broad diffuse peaks, commonly observed in amorphous solids,<sup>2</sup> dominate the x-ray patterns while other remaining x-ray-diffraction peaks broaden, decline in intensity and vanish. At pressures in excess of 10 GPa as seen in Figs. 3(a) and 3(b), the  $K_2ZnCl_4$  and  $Rb_2ZnCl_4$  isomorphs rapidly converge on x-ray amorphous states.  $Cs_2ZnCl_4$ , despite its intimate structural and chemical similarity to its two isomorphs behaves differently. The clustering of peaks in its spectrum is a precursor not to an amorphous structure, but to a high-pressure crystalline phase, whose x-ray-diffraction pattern above 14.0 GPa can no longer be indexed on the basis of the ambient pressure orthorhombic ( $Pnma$ ) structure. This diffraction pattern remains crystalline to the highest pressures measured, approaching 60 GPa [Fig. 3(c)]. The fact that the three isomorphs essentially differ only via the tetrahedral  $BX_4$  unit to  $A$  cation size ratio, indicates that this ionic size ratio dictates the tendency of these solids to either undergo a crystal-crystal phase transition at pressure, or become impeded in their effort to do so, resulting in intermediate amorphous phases. To consolidate this finding we extended our examination to two other isomorphs in this family. The fourth isomorph in our study,  $K_2SeO_4$ , has a  $BX_4/A$  ratio of (1.23) below that of  $Cs_2ZnCl_4$ . Consistent with the emerging ionic size ratio systematic, its behavior mirrors that of its  $Cs_2ZnCl_4$  isomorph [Fig. 3(d)]. Between 8 and 17 GPa as indicated by the arrow in the figure, an initial

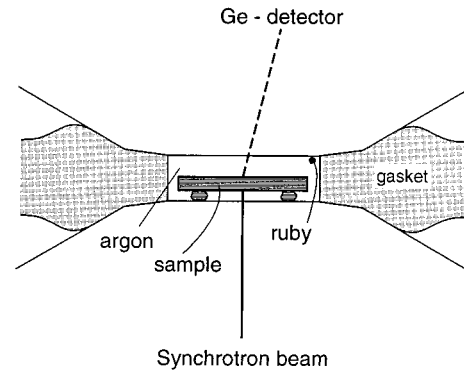


FIG. 2. Schematic of the diamond cell assemblage, used for compressing  $K_2ZnCl_4$  and  $Rb_2ZnCl_4$  in an argon medium.

conglomeration of peaks develops which is a precursor to a crystalline phase emerging at higher pressures, and remaining crystalline to the highest pressures measured approaching 60 GPa. We then considered  $Rb_2ZnBr_4$  ( $BX_4/A = 1.62$ ), characterized by an ionic size ratio between that of  $K_2ZnCl_4$  (1.69) and  $Rb_2ZnCl_4$  (1.52). Since the latter two isomorphs become amorphous upon compression any other member of this family with a size ratio intermediate between these two should exhibit the same behavior. The effect of pressure on the x-ray-diffraction pattern of  $Rb_2ZnBr_4$  reflects this trend. At lower pressures the spectrum undergoes a marked decrease in the intensity of the various diffraction peaks with the simultaneous emergence of a ‘‘halolike’’ feature at  $\sim 14$  GPa as indicated by the arrow in Fig. 3(e). At higher pressures this broad diffuse peak dominates the pattern and  $Rb_2ZnBr_4$  rapidly converges on an x-ray amorphous phase. Note also the return of the diffraction features for this and the other isomorphs upon release of pressure, albeit with some intensity variations, consistent with the displacive character of these transitions for nondirectionally bonded solids. We additionally examined the compressional behavior of  $Cs_2ZnBr_4$  which is characterized by an anion to cation size ratio ( $ZnBr_4/Cs^+ = 1.43$ ) between that of the isomorphs that amorphize and those that do not. Strikingly this system, as seen in Fig. 3(f), exhibits behavior intermediate between that of the former and latter isomorphs. While its x-ray-diffraction pattern develops a characteristic broad diffuse peak at about 11 GPa, indicated by an arrow in the figure, the crystal does not converge either on a high-pressure crystal phase or on an amorphous phase. Rather it retains to the highest pressure measured – 64 GPa, the basic features that emerged at 11 GPa, namely a ‘‘halolike structure,’’ on which broadened x-ray-diffraction peaks are superimposed. Finally we have also documented the amorphization of  $K_2ZnCl_4$  and  $Rb_2ZnCl_4$  in an argon medium [Figs. 4(a) and 4(b)] confirming that the order-disorder transitions are not due to any deviatoric stress in the sample.

#### IV. DISCUSSION

These results indicate that the  $BX_4/A$  size ratio criterion is effective in predicting whether crystals in this family will undergo a crystal-crystal phase transition at pressure or whether such a transition will be impeded resulting in an amorphous phase. Consequently based on our study, crystals

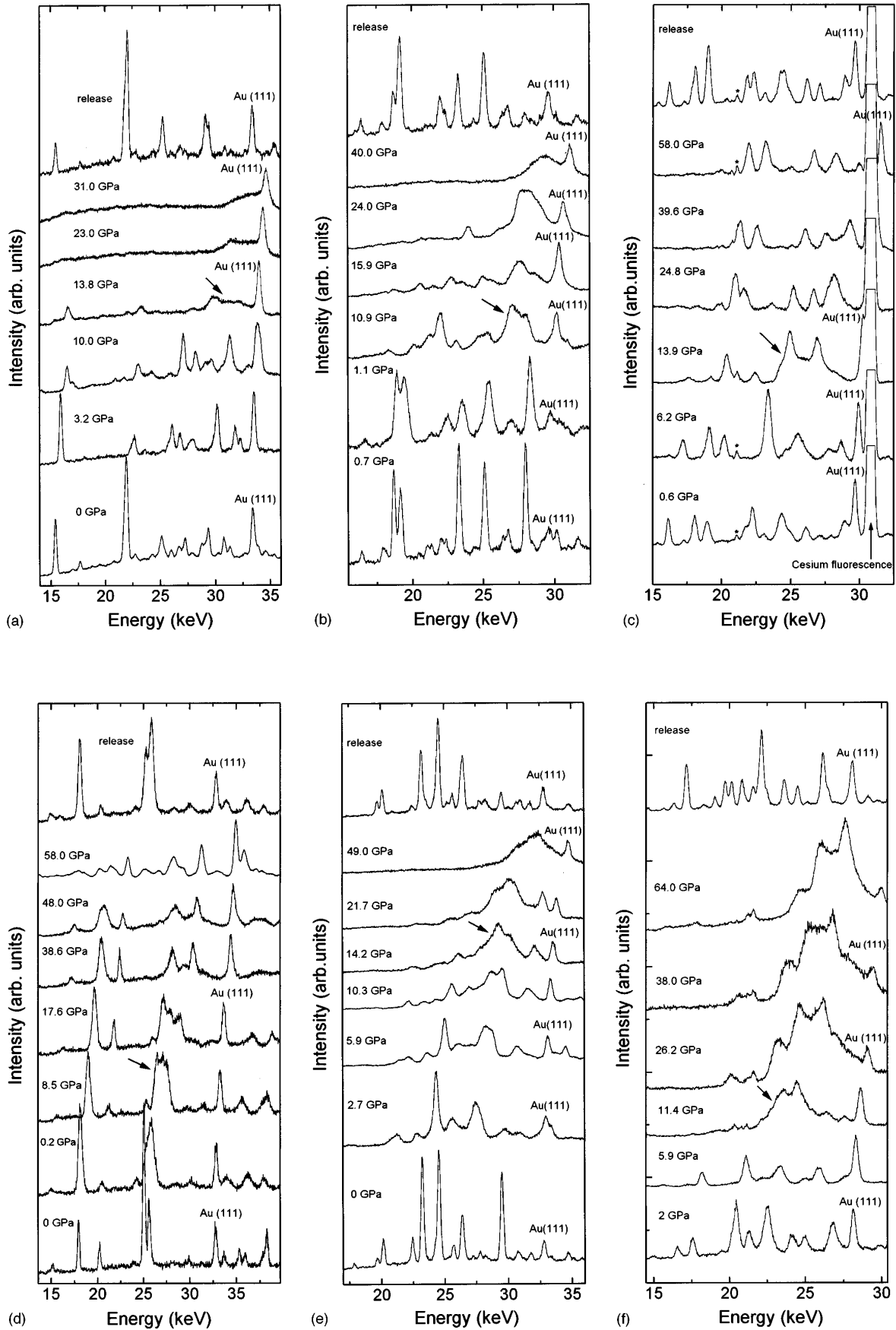


FIG. 3. Energy-dispersive x-ray-diffraction measurements on  $K_2ZnCl_4$  (a),  $Rb_2ZnCl_4$  (b),  $Cs_2ZnCl_4$  (c),  $K_2SeO_4$  (d),  $Rb_2ZnBr_4$  (e),  $Cs_2ZnBr_4$  (f) at various pressures. The features labeled with an asterisk in (c) are escape peaks due to the intense cesium fluorescence.

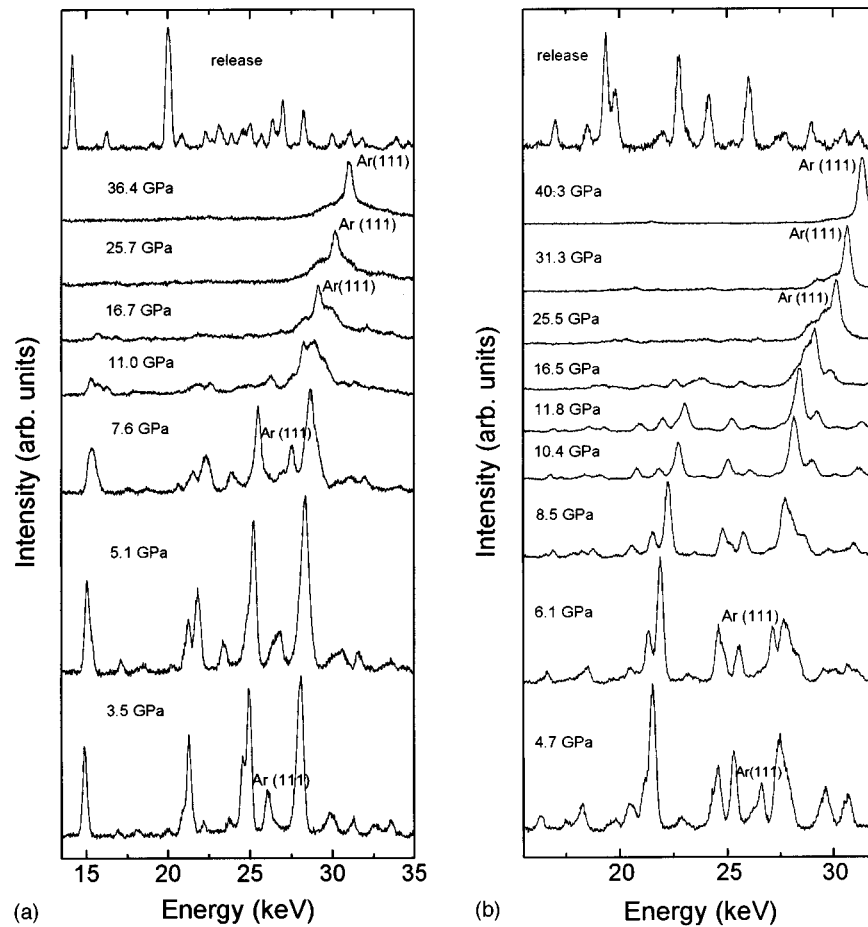


FIG. 4. Energy-dispersive x-ray-diffraction measurements of  $K_2ZnCl_4$  (a) and  $Rb_2ZnCl_4$  (b) in an argon medium.

with  $BX_4/A$  size ratios below that of  $Cs_2ZnBr_4$  will transform to a high-pressure crystalline phase whereas crystals with  $BX_4/A$  ratios above that of  $Cs_2ZnBr_4$  will transform to noncrystalline solids upon compression, while  $Cs_2ZnBr_4$  with its intermediate size ratio bridges the contrasting behavior of its isomorphs. This criterion effectively applies to other classes of molecular solids such as the simpler  $BX_4$  family where  $B=Sn, Ge$  and  $X=I, Br, Cl$ .<sup>2</sup> In these structures the interstitial sites between the  $BX_4$  tetrahedral units are empty. Therefore the  $BX_4$  to “A” ratio may be viewed as very large or infinite and the crystals are apt to amorphize upon compression. This is consistent with the already observed amorphization of all examined members of this family at pressures above 8 to 10 GPa.<sup>2,21–24</sup>

There are distinct analogies between the ionic size ratio systematics identified here for crystalline to noncrystalline transitions and those found to dictate crystal-crystal phase transitions in a variety of simpler system such as alkali halides. For example in sodium halides, NaF and NaCl undergo the well documented  $B1-B2$  transition at pressure.<sup>25</sup> When the anion to cation size ratio though is larger as is true for the NaBr and NaI isomorphs the crystals do not undergo the  $B1-B2$  transition but rather transform to a distorted B1 structure upon compression. For these crystals it was indicated that when the anion to cation size ratio exceeds a threshold value the B1 phase becomes denser than the hypothetical B2 phase, resulting in a transition to a distorted B1

phase upon compression instead.<sup>25</sup> This reasoning likely explains the transition to a noncrystalline state for the more complex  $A_2BX_4$  salts when  $BX_4/A$  ratios exceed a critical value. We can also view the transitions in terms of a packing of the anionic  $BX_4$  units around the A cations. When the  $BX_4$  (for example  $ZnCl_4$ ) units are small relative to the A cations (for example  $Cs^+$ ) increasing repulsive and steric stresses induced by pressure can be accommodated by deformations of the  $Cs^+$  outer shell as opposed to significant changes in its average position. In contrast to this smaller A cations such as  $K^+$  will accommodate increased stresses through larger and more varied displacements from their average positions resulting in a subsequent loss of translational periodicity at high pressures. This view is consistent with the explanation provided for the incommensurate lattice instabil-

TABLE II. Link between ionic size ratios of several  $A_2BX_4$  halide isomorphs and their incommensurate and high-pressure phase behavior (Refs. 15 and 16).

$A_2BX_4$	$BX_4/A$	Incommensurate phase	Amorphous phase
$K_2ZnCl_4$	1.691	Yes	Yes
$Rb_2ZnBr_4$	1.616	Yes	Yes
$Rb_2ZnCl_4$	1.521	Yes	Yes
$Cs_2ZnBr_4$	1.431	No	No
$Cs_2ZnCl_4$	1.347	No	No

ity exhibited by several of these compounds at ambient pressure.<sup>13–15,26</sup> It was found that the presence of large anionic  $BX_4$  groups in relation to the size of the  $A$  cations induces increased stresses in the backbone lattice resulting in an incommensurate modulation and strict loss of translational periodicity along a particular crystallographic axis. Notably (see Table II) the  $BX_4/A$  size threshold above which an incommensurate modulation arises for halides in this family is correlated with that found here above which a crystalline to noncrystalline transition occurs. This then points to a common structural criterion governing order-disorder transitions in this family.

Incommensurate solids constitute in many respects a structural bridge between amorphous solids and crystals since they are characterized both by translational order and aperiodicity. This sets the stage for further sensitive light

scattering and angle-dispersive x-ray-diffraction experiments to investigate, for example, whether transitions from the crystalline to the noncrystalline state can be mediated by a transitional incommensurate phase. More generally identifying criteria such as the ionic size ratio found in this study for predicting the transition from the ordered to the disordered state for extended structural families constitutes a significant step towards unraveling the mechanism of formation and underlying structure of disordered solids.

#### ACKNOWLEDGMENTS

We thank J. Otto for valuable advice and assistance with the x-ray-diffraction measurements and O. Tschauer and A. Zerr for helpful discussions.

- 
- <sup>1</sup>S. R. Elliott, *Physics of Amorphous Materials*, 2nd ed. (Longman, Essex, United Kingdom, 1990).
- <sup>2</sup>Y. Fujii, M. Kowaka, and A. Onodera, *J. Phys. C* **18**, 789 (1985).
- <sup>3</sup>K. J. Kingma, C. Meade, R. J. Hemley, H. K. Mao, and D. R. Veblen, *Science* **259**, 666 (1993).
- <sup>4</sup>G. C. Serghiou, R. R. Winters, and W. S. Hammack, *Phys. Rev. Lett.* **68**, 3311 (1992).
- <sup>5</sup>O. Mishima, L. D. Calvert, and E. Whalley, *Nature (London)* **310**, 393 (1984).
- <sup>6</sup>R. R. Winters and W. S. Hammack, *Science* **260**, 202 (1993).
- <sup>7</sup>M. Hemmati, A. Chizmeshya, G. H. Wolf, P. H. Poole, S. Shao, and C. A. Angell, *Phys. Rev. B* **51**, 14 841 (1995).
- <sup>8</sup>M. B. Kruger, Q. Williams, and R. Jeanloz, *J. Chem. Phys.* **91**, 5910 (1989).
- <sup>9</sup>J. S. Tse, D. D. Klug, J. A. Ripmeester, S. Desgreniers, and K. Lagarec, *Nature (London)* **369**, 724 (1994).
- <sup>10</sup>L. C. Ming and A. Jayaraman, *J. Phys. Chem. Solids* **57**, 247 (1996).
- <sup>11</sup>H. M. Lu and J. R. Hardy, *Phys. Rev. B* **45**, 7609 (1992).
- <sup>12</sup>J. R. Hardy, *Ferroelectrics* **117**, 53 (1991).
- <sup>13</sup>I. Etzbarria, J. M. Perez-Mato, and G. Madariaga, *Phys. Rev. B* **42**, 8482 (1990).
- <sup>14</sup>I. Etzbarria, J. M. Perez-Mato, and G. Madariaga, *Phys. Rev. B* **46**, 2764 (1992).
- <sup>15</sup>H. Z. Cummins, *Phys. Rep.* **185**, 211 (1990).
- <sup>16</sup>B. Brehler, *Z. Kristallogr.* **109**, 68 (1957); B. Morosin and E. C. Lingafelter, *Acta Crystallogr. B* **12**, 744 (1959); A. Kalman, J. S. Stephens, and D. W. J. Cruickshank, *ibid.* **26**, 1451 (1970); J. Lamotte and J. Vermeire, *J. Appl. Crystallogr.* **8**, 689 (1975); P. T. T. Wong, *J. Chem. Phys.* **66**, 2347 (1977); C. J. Pater, *Acta Crystallogr. B* **35**, 299 (1979); M. Quilchini and J. Pannetier, *ibid.* **39**, 657 (1983); V. Katkanant and J. R. Hardy, *Ferroelectrics* **82**, 185 (1988); V. Katkanant, J. R. Hardy, R. D. Kirby, and F. G. Ullman, *ibid.* **99**, 213 (1989).
- <sup>17</sup>H. K. Mao, J. Xu, and P. M. Bell, *J. Geophys. Res.* **91**, 4673 (1986).
- <sup>18</sup>D. L. Heinz and R. Jeanloz, *J. Appl. Phys.* **55**, 885 (1984); P. Richet, Ji-An Xu, and Ho-Kwang Mao, *Phys. Chem. Mineral* **16**, 207 (1988).
- <sup>19</sup>Pressure was determined with the ruby-fluorescence method, the equation of state of gold or that of argon. Both ruby and gold and argon were used to monitor pressure to about 30 GPa. The pressures determined by these two methods were within 1 GPa of each other in agreement with previous work (Ref. 18). At higher pressures, where the pressure gradients from the center to the edge of the gasket hole increase, the equation of state of gold or argon was used since they were in intimate contact with the  $40 \times 40 \mu\text{m}$  sampled region of the solid whereas the ruby chips were located near the edge of the gasket hole. The x-ray patterns are normalized to the intensity of their gold (111) or argon (111) diffraction peaks.
- <sup>20</sup>The samples were grown by slow evaporation of aqueous solutions containing stoichiometric amounts of the component  $AX$  and  $BX_2$  starting materials at room temperature.
- <sup>21</sup>S. Sugai, *J. Phys. C* **18**, 799 (1985).
- <sup>22</sup>A. L. Chen, P. Y. Yu, and M. P. Pasternak, *Phys. Rev. B* **44**, 2883 (1991).
- <sup>23</sup>W. Williamson III and S. A. Lee, *Phys. Rev. B* **44**, 9853 (1991).
- <sup>24</sup>G. R. Hearne, M. P. Pasternak, and D. R. Taylor, *Phys. Rev. B* **52**, 9209 (1995).
- <sup>25</sup>T. Yagi, T. Suzuki, and S. Akimoto, *J. Phys. Chem. Solids* **44**, 135 (1983).
- <sup>26</sup>V. Katkanant, P. J. Edwardson, J. R. Hardy, and L. L. Boyer, *Phase Transitions* **15**, 103 (1989).